ATM activation by a sulfhydryl-reactive inflammatory cyclopentenone prostaglandin

doi: 10.1111/j.1365-2443.2006.00976.x

ATM Activation by a Sulfhydryl-Reactive Inflammatory Cyclopentenone Prostaglandin

Masahiko Kobayashi[1], Hirohito Ono[1], Keiko Mihara[1], Hiroshi Tauchi[2], Kenshi Komatsu[3], Takashi Shibata[4], Hiroko Shimizu[1], Koji Uchida[4], and Ken-ichi Yamamoto[1]

[1]Department of Molecular Pathology, Cancer Research Institute, Kanazawa University, Kanazawa, 13-1 Takaramachi, Ishikawa 920-0934, Japan, [2]Department of Environmental Science, Faculty of Science, Ibaraki University, 2-1-1 Bunkyo, Mito, Ibaraki 310-8512, Japan, [3]Radiation Biology Center, Kyoto University, Yoshida Konoe, Sakyo-ku, Kyoto 606-8501, Japan, and [4]Graduate School of Bioagricultural Science, Nagoya University, Nagoya464-8601, Japan.

Running title: ATM activation by cyclopentenone prostaglandins

Address correspondence to: Ken-ichi Yamamoto, Department of Molecular Pathology, Cancer Research Institute, Kanazawa University, Kanazawa, 13-1 Takaramachi, Ishikawa 920-0934, Japan. Tel, 81-76-265-2755; Fax, 81-76-234-4517; e-mail, kyamamot@kenroku.kanazawa-u.ac.jp

Abstract

ATM (ataxia-telangiectasia mutated) is activated by a variety of noxious agent, including oxidative stress, and ATM deficiency results in an anomalous cellular response to oxidative stress. However, the mechanisms for ATM activation by oxidative stress remain to be established. Furthermore, it is not clear whether ATM responds to oxidative DNA damage or to a change in the intracellular redox state, independent of DNA damage. We found that ATM is activated by N-methyl-N'-nitro-nitrosoguanidine (MNNG) and 15-deoxy-Δ12,14-prostaglandin J_2 (15d-PGJ_2), in *NBS1*- or *MSH6*- deficient cells. We further found that ATM is activated by treating chromatin-free immunoprecipitated ATM with MNNG or 15d-PGJ_2, which modifies free sulfhydryl (SH) groups, and that 15d-PGJ_2 binds covalently to ATM. Interestingly, 15d-PGJ_2-induced ATM activation leads to p53 activation and apoptosis, but not to Chk2 or H2AX phosphorylation. These results indicate that ATM is activated through the direct modification of its SH groups, independent of DNA damage, and this activation leads, downstream, to apoptosis.

Introduction

Ataxia-telangiectasia (A-T) is an autosomal recessive disorder with pleiotropic clinical phenotypes, including progressive cerebellar ataxia, oculocutaneous telangiectasias, immune deficiencies, premature aging, gonadal dysgenesis, growth retardation, and a high incidence of lymphoid malignancies. Cells derived from A-T patients are characterized by genomic instability and extreme sensitivity to ionizing radiation (IR). In response to IR, they fail to arrest during DNA synthesis or to stop at the G1/S or G2/M cell-cycle checkpoints, suggesting these cellular anomalies are a major underlying cause of the disease. The 350-KDa product of the gene mutated in A-T (designated *ATM*) is closely related to the yeast checkpoint proteins Rad3 and Mec1. These proteins form a family of large protein kinases characterized by a carboxy-terminal phosphatidylinositol (PI)-3 kinase-like domain, and play essential roles in DNA repair and cell-cycle checkpoint control by phosphorylating key downstream molecules. Many recent studies have established that vertebrate ATM acts on a number of effector proteins following IR, notably p53, Chk2, and c-Abl, which is consistent with ATM being a major regulator of the cellular response to IR-generated DNA damage (Shiloh and Kastan, 2001). In addition, ATM is involved in homologous recombinational DNA repair, an essential DNA repair system for double-strand breaks (DSB) in the DNA of vertebrate cells (Morrison et al., 2000). ATM is thus specifically involved in cellular responses to DSB DNA damage in vertebrate cells. On the other hand, ATR (ATM-Rad3 related), another vertebrate family member that is even more closely related to Rad3/Mec1, plays an essential role in checkpoint responses to hydroxyurea, UV, cisplatin, 4-nitroquinolin, or other agents, which do not induce DSB directly, but rather cause DNA replication to stall (Abraham, 2001).

The results of several recent studies indicate that ATM is activated by a variety of noxious agents, such as alkylating agents, oxidative stress, poly-Q aggregates, and UVA (Adamson et al., 2002; Giuliano et al., 2003; Shackelford et al., 2001; Zhang et al., 2002), which may not directly generate DSB. Furthermore, it is now clear that the loss of ATM results in an anomalous cellular response to oxidative stress. This includes decreased levels of catalase activity, increased levels of lipid

hydroperoxides, reduced levels of cyclic nucleotides such as NADH and NADPH, enhanced generation of reactive oxygen species, enhanced heme oxygenase mRNA expression, and increased levels of oxidant-modified proteins and lipids in *ATM*-deficient cells lines or tissues, including the brain of *ATM* knockout mice (Barlow et al., 1999; Kamsler et al., 2001; Stern et al., 2002; Takao et al., 2000). More recently, impaired self-renewal of hematopoietic stem cells in *ATM* knockout mice has been attributed to the defective response to oxidative stress (Ito et al., 2004). Thus, the defective response to oxidative stress may underlie the pathogenesis of some of the clinical phenotypes of A-T, such as cerebellar ataxia, premature aging, growth retardation, and cancer predisposition. Nonetheless, it remains to be established how ATM is activated by oxidative stress or other noxious agents that may not directly induce DSB. Furthermore, the molecular mechanisms underlying the apoptosis of postmitotic cerebellar Purkinje cells, which is responsible for cerebellar ataxia, have remained elusive.

A reactive cyclopentenone-type prostaglandin (15-deoxy-D12,14-prostaglandin J_2, 15d-PGJ_2) is a prostaglandin D_2 metabolite generated during inflammatory processes that is, due to the presence of a reactive □,□-unsaturated ketone in the cyclopentenone ring, a potent inducer of intracellular oxidative stress (Gilroy et al., 1999; Kondo et al., 2001; Shibata et al., 2002). Furthermore, 15d-PGJ_2 has been shown to directly modulate the activity of several biologically important molecules, such as NF-□B, □□□ kinase, H-Ras, and thioredoxin, through the specific alkylation of free sulfhydryl (SH) groups on cysteine residues of the target proteins (Cernuda-Morollon et al., 2001; Oliva et al., 2003; Rossi et al., 2000; Shibata et al., 2003). An alkylating agent, N-methyl-N'-nitro-nitrosoguanidine (MNNG), is another potential oxidative stress inducer (Reitman et al., 1988) that reacts with free SH groups (Johnson and Greenberg, 1973; Nagao et al., 1971; Sugimura et al., 1968), although MNNG is well known to methylate DNA (e.g., O^6-methylguanine (O^6-MeG)) (Stojic et al., 2004a), and effectively induces checkpoint activation through the activation of both ATM and ATR with the subsequent activation of Chk1 and Chk2 (Beardsley et al., 2005; Stojic et al., 2004b; Wang and Qin, 2003).

Here, we used these two agents to study whether ATM responds to the oxidative or methylation damage of DNA or, rather, to a change in the intracellular redox state, independent of DNA damage.

To address this issue specifically, we used *NBS1*- and *MSH6*-deficient cells that were generated by targeted disruption. Nbs1 forms an evolutionarily conserved complex with Mre11 and Rad50, in which Nbs1 interacts with ATM and recruits it to DSB sites. Nbs1 is essential for DSB-induced ATM activation and the subsequent phosphorylation of ATM target proteins, such as Nbs1 itself, Chk2, and SMC1, in vertebrate cells (Falck et al., 2005; Kitagawa et al., 2004; Lee and Paull, 2004; Lee and Paull, 2005; Uziel et al., 2003). Msh6 and Msh2 form an evolutionarily conserved mismatch repair complex (MutS□). They recognize methylated DNAs such as O^6-MeG (Stojic et al., 2004a) and are required for MNNG-induced ATR activation and Chk1 phosphorylation by ATR (Stojic et al., 2004b; Wang and Qin, 2003). In the present study, we found that ATM is activated by MNNG and 15d-PGJ_2 in an Nbs1- and Msh6-independent manner. We further found that ATM is activated by the direct treatment of chromatin-free immunoprecipitated ATM with MNNG or 15d-PGJ_2, through the modification of SH groups on ATM, and that 15d-PGJ_2 covalently binds to ATM. Interestingly, 15d-PGJ_2-induced ATM activation leads to the phosphorylation and accumulation of p53 and to apoptosis, but not to Chk2 or H2AX phosphorylation in human tumor cells. These results indicate that ATM is directly activated by free SH-group-modifying agents and thereafter induces a distinct downstream response.

Results

MNNG activates ATM in an Nbs1- and Msh6-independent manner. To study the mechanisms by which MNNG activates the ATM kinase, we developed an IP kinase assay for ATM in chicken DT40 cells, using anti-chicken ATM antibodies. The rational for using DT40 cells was the availability of a panel of stable isogenic knockout cell lines, including *ATM*$^{-/-}$, *NBS1*$^{-/-/-}$, *RAD17*$^{-/-}$, *RAD9*$^{-/-}$, and *MSH6*$^{-/-}$ lines (Kobayashi et al., 2004; Takao et al., 1999; Tauchi et al., 2002)(Supplementary Fig. 1). However, since the human ATM autophosphorylation site (Ser-1981) (Bakkenist and Kastan, 2003) is not conserved in chicken ATM (Supplementary Fig. 2), and since some agents such as okadaic acid (OA) induce ATM autophosphorylation on Ser-1981 but not ATM kinase activation (Goodarzi et al.,

2004), we adopted the IP ATM kinase assay to measure ATM activation. In this kinase assay, a GST-chicken Rad9 fusion protein rather than a PHAS-1 artificial substrate was used as the substrate for the chicken ATM kinase, because a region containing an ATM phosphorylation site corresponding to Ser-272 in human Rad9 (Chen et al., 2001) is well conserved in chicken Rad9 (Kobayashi et al., 2004) (Supplementary Fig. 3) and because this fusion protein gives more reliable results than PHAS-1, with low background. Using this ATM IP kinase assay, we confirmed that Nbs1 is required for effective IR-induced ATM activation (Supplementary Fig. 4) (Falck et al., 2005; Kitagawa et al., 2004; Uziel et al., 2003). Having established the ATM kinase assay in DT40 cells, we then analyzed the activation of ATM kinase in wild-type DT40 cells treated with various concentrations of MNNG. As shown in Fig. 1A, the ATM kinase was effectively activated with MNNG; the maximum activation of ATM was observed with 200 μM MNNG for 1 hr, though 10 μM MNNG was sufficient to kill 99% DT40 cells (data not shown). However, higher concentrations of MNNG were rather inhibitory for ATM kinase activity, as we found that excess SH modification of ATM is inhibitory (see also Fig.2).

If some DNA lesions caused by MNNG, such as O^6-MeG, generate DSB through DNA repair or replication and then activate ATM, *NBS1*-deficient cells should show an impaired ATM response to MNNG. To test this hypothesis, we treated *NBS1*$^{-/-}$ cells with MNNG and examined ATM activation and the phosphorylation of Chk1 (Ser-345) and Chk2 (Thr-68). A recent study showed that Nbs1, in addition to its role in DSB-induced ATM activation, is involved in the ATR-mediated Chk1 phosphorylation induced by HU and UV (Stiff et al., 2005). Consistent with these findings, the MNNG-induced Chk1 phosphorylation on Ser-345 was severely diminished in *NBS1*$^{-/-}$ cells (Fig. 1B).
In the wild-type cells, we also observed MNNG-induced Chk2 phosphorylation (Fig. 1B), which was previously shown to be independent of human ATM and of Mlh1 mismatch repair proteins, particularly at higher MNNG concentrations (Beardsley et al., 2005), such as those used in the present study (see also Fig. 1D and Fig. 5B). However, as shown in Fig. 1B, we observed greatly reduced MNNG-induced Chk2 phosphorylation in *NBS1*$^{-/-}$ cells, indicating that ATM and mismatch repair proteins are dispensable, but Nbs1 is required for the Chk2 phosphorylation induced by high concentrations of MNNG. Fig. 1C shows that, despite the requirement for Nbs1 for MNNG-induced

Chk1 and Chk2 phosphorylation, MNNG effectively induced ATM kinase activation in *NBS1*$^{-/-}$ cells, the degree of which was comparable to the level observed in wild-type cells. These results indicate that, in contrast to the MNNG-induced phosphorylation of Chk1 and Chk2, which is dependent on Nbs1, MNNG-induced ATM kinase activation is independent of Nbs1.

MutS□, which consists of Msh2 and Msh6, is known to bind the O^6-MeG generated by MNNG and is involved in the ATR-mediated Chk1 phosphorylation induced by MNNG (Stojic et al., 2004b), through direct interactions with ATR (Wang and Qin, 2003). As shown in Fig. 1D, we confirmed the requirement for Msh6 for MNNG-induced and ATR-mediated Chk1 phosphorylation. However, we observed that the ATM kinase was effectively activated in *MSH6*$^{-/-}$ cells in response to MNNG (Fig. 1E), in agreement with previous findings that MNNG induces the activation of ATM kinase in human *MLH1*-deficient HCT116 cells (Adamson et al., 2002). In addition, O^6-benzyl guanine, a specific inhibitor for methylguanine methyltransferase, neither inhibited nor enhanced MNNG-induced ATM activation (data not shown).

ATM is directly activated by MNNG through the modification of free SH groups

The above results, showing that MNNG-induced ATM kinase activation requires neither Nbs1 nor Msh6 (Fig. 1), raise the possibility that MNNG acts directly on ATM, rather than through the generation of methylated DNA. To explore this possibility, immunoprecipitated ATM, prepared from untreated DT40 cells with antibodies specific for chicken ATM, was treated with MNNG, and the ATM kinase activity was measured. As shown in Fig. 2A, ATM was significantly activated by MNNG in this chromatin-free experiment, and much lower concentrations of MNNG (0.2 □M) were sufficient for the maximum activation of ATM activity. These results further support the possibility that MNNG acts directly on ATM rather than through the generation of methylated DNA. Since, in addition to methylating DNA, MNNG modifies SH groups on cysteine residues in some proteins (Johnson and Greenberg, 1973; Nagao et al., 1971; Sugimura et al., 1968), we investigated whether the MNNG-mediated modification of ATM's SH groups is involved in the cell-free activation of ATM by MNNG. Immunoprecipitated ATM was therefore pre-treated with a SH-specific agent, N-ethylmaleimide (NEM), before MNNG treatment. As shown in Fig. 2B, the activation of ATM by 0.5 □M MNNG was

completely inhibited by the pre-treatment with excess NEM (1 mM). Furthermore, the basal activity of ATM decreased after pre-treatment with high concentrations of NEM (4 mM), indicating that excess SH modification is inhibitory for the ATM kinase activity. These results suggest that ATM is activated by MNNG through the modification of critical SH groups in ATM, independent of DNA modification, and that excess SH modification is rather inhibitory for the ATM kinase activity.

15d-PGJ$_2$ covalently binds and activates ATM

Because SH groups seemed to be important for the direct activation of the ATM kinase by MNNG (Fig. 2B), we studied whether another specific SH-reactive oxidative stress inducer, 15d-PGJ$_2$, would induce ATM kinase activation. DT40 cells were treated with various concentrations of 15d-PGJ$_2$ for 1 h, and the ATM kinase activity was measured. As shown in Fig. 3A, ATM was effectively activated with 20 □M of 15d-PGJ$_2$, and this 15d-PGJ$_2$-induced ATM activation was observed in *NBS1*$^{-/-}$ DT40 cells (data not shown). However, ATM activation was not observed with 9,10-dihydro-15d-PGJ$_2$ (CAY, Fig. 3B). This 15d-PGJ$_2$ analog, unlike 15d-PGJ$_2$, lacks an electrophilic □,□-unsaturated ketone, and therefore can neither function as an oxidative stress inducer nor react with the SH groups of target proteins (Shibata et al., 2003). Interestingly, we did not detect significant Chk1, Chk2 and H2AX phosphorylation in cells treated with 15d-PGJ$_2$ (data not shown, see also Fig. 5A and 5C), although MNNG effectively induced Chk1, Chk2 and H2AX phosphorylation along with ATM kinase activation (Fig. 1 and 5). We then treated immunoprecipitated ATM, prepared from untreated cells, with 15d-PGJ$_2$, and measured the ATM kinase activity. The results, shown in Fig. 3C, indicate that, similar to the MNNG treatment, the ATM kinase was also effectively activated by the direct treatment of immunoprecipitated ATM with low concentrations of 15d-PGJ$_2$ (0.2 nM).

Because 15d-PGJ$_2$ directly modulates the biological activities of NF-□B, □□□ kinase, H-Ras, and thioredoxin through covalent binding to specific cysteine residues (Cernuda-Morollon et al., 2001; Oliva et al., 2003; Rossi et al., 2000; Shibata et al., 2003), we used biotinylated 15d-PGJ$_2$ to investigate whether 15d-PGJ$_2$ binds to ATM. Immunoprecipitates prepared from wild-type or *ATM*$^{-/-}$ DT40 cells with antibodies specific to chicken ATM were treated with 50 □M biotinylated 15d-PGJ$_2$ and then immunoblotted with HRP-conjugated NeutrAvidin. As shown in Fig. 4A, biotinylated 15d-

PGJ_2 bound to ATM was detected in the immunoprecipitates prepared from wild-type but not *ATM*$^{-/-}$ DT40 cells. In addition, we analyzed 15d-PGJ_2 binding to HA-tagged human ATM (HA-hATM). HA-hATM was induced with doxycycline in *ATM*$^{-/-}$ DT40 cells stably expressing inducible HA-hATM (*ATM*$^{-/-}$/HA-hATM), and was immunoprecipitated with anti-HA antibodies. The immunoprecipitated HA-hATM was then treated with biotinylated 15d-PGJ_2, and the 15d-PGJ_2 binding to HA-hATM was determined by immunoblot analysis with HRP-conjugated NeutrAvidin. Similar to chicken ATM, we detected biotinylated 15d-PGJ_2 bound to HA-hATM only when the immunoprecipitates were prepared from cells in which the HA-hATM expression was induced by doxycycline (Fig. 4B). In another experiment, we treated *ATM*$^{-/-}$/HA-hATM cells with biotinylated 15d-PGJ_2 after HA-hATM induction. Biotinylated 15d-PGJ_2-binding proteins were then precipitated with NeutrAvidin Plus beads, and both the precipitates ("Bound") and the supernatants ("Unbound") were immunoblotted with anti-HA. As shown in Fig. 4C, while HA-hATM was found exclusively in the "Unbound" fraction in the absence of treatment with biotinylated 15d-PGJ_2, all the HA-hATM was detected in the "Bound" fraction after treatment with biotinylated 15d-PGJ_2. The results of these experiments demonstrate that 15d-PGJ_2 binds to ATM, presumably through the alkylation of ATM's cysteine residues.

15d-PGJ_2 induces p53 phosphorylation and apoptosis in an ATM-dependent manner

Since 15d-PGJ_2 effectively activated the ATM kinase, it was important to investigate the possible functional consequences of ATM activation by 15d-PGJ_2. However, we could not study one of the important ATM target molecules, p53 (Shiloh and Kastan, 2001), in DT40 cells, because p53 expression is extremely low in these cells (Takao et al., 1999), and the ATM phosphorylation site in the N-terminal region of p53 is not conserved in chicken p53 (Soussi T, 1988). In addition, the phosphorylation of Chk1, Chk2 and H2AX was not observed in DT40 cells in response to 15d-PGJ_2 (data not shown). We therefore analyzed the phosphorylation of p53 (Ser-15) and Chk2 (Thr-68) in the YZ5 (*ATM*+) and EBS (*ATM*-) human cell lines (Ziv et al., 1997) following treatment with 15d-PGJ_2. As shown in Fig. 5A, 15d-PGJ_2 induced p53 phosphorylation in the YZ5 cells but not the EBS cells, establishing that ATM-dependent phosphorylation of p53 is induced by 15d-PGJ_2. However, the phosphorylation of Chk2 (Fig. 5A) was not detected in either cell line, just as in the DT40 cells. On

the other hand, IR effectively induced the phosphorylation of both Chk2 and p53 in the YZ5 cells, and the degree of phosphorylation of both proteins was much lower in the EBS cells (Fig. 5B), confirming the inductions of ATM-dependent p53 and Chk2 phosphorylation by IR. However, MNNG effectively induced the phosphorylation of Chk2 and p53 in both the YZ5 and EBS cells, indicating that MNNG-induced p53 or Chk2 phosphorylation is only partially dependent on ATM. Since we could not detect ATM autophosphorylation on Ser-1981 in YZ5 cells following IR treatment, due to the extremely low ATM expression in the YZ5 line, we studied ATM autophosphorylation and H2AX phosphorylation (Ser-139) along with p53 phosphorylation in MCF7 cells. As shown in Fig. 5C, 15d-PGJ_2 (40 □M) induced only a marginal degree of ATM autophosphorylation, though 15d-PGJ_2 was effective in p53 phosphorylation and accumulation. In addition, we could not detect significant H2AX phosphorylation following the 15d-PGJ_2 treatment, even though MNNG was very effective in phosphorylating H2AX (Fig. 5C). This result is consistent with previous findings that agents that alter chromatin structure without introducing detectable DSB induce ATM autophosphorylation but not H2AX phosphorylation (Bakkenist and Kastan, 2003).

Because ATM activation and p53 phosphorylation were observed in response to 15d-PGJ_2, we investigated whether 15d-PGJ_2 induces ATM-dependent apoptosis in human cells. YZ5 and EBS cells were treated with 40 □M of 15d-PGJ_2 for 24 h, and apoptotic cells were quantified using annexin V FACS analysis. The results shown in Fig. 5D indicate that 15d-PGJ_2 induces ATM-dependent apoptosis in human tumor cells.

Discussion

ATM is activated by DSB and is essential for the cellular response to DSB in vertebrate cells (Shiloh and Kastan, 2001). ATM is also activated by a variety of noxious agents, such as alkylating agents, oxidative stress, poly-Q aggregates, and UVA (Adamson et al., 2002; Giuliano et al., 2003; Shackelford et al., 2001; Zhang et al., 2002), which may not directly generate DSB. Furthermore, ATM deficiency results in an anomalous cellular response to oxidative stress (Barlow et al., 1999; Ito

et al., 2004; Kamsler et al., 2001; Stern et al., 2002; Takao et al., 2000). While this defective response to oxidative stress may underlie the pathogenesis of cerebellar ataxia, premature aging, growth retardation, or cancer predisposition in A-T, the mechanisms for ATM activation by oxidative stress or other noxious agents remain to be determined. Furthermore, it is not clear whether or not ATM responds to oxidative DNA damage or to a change in the intracellular redox state, independent of DNA damage. To address these issues, we studied ATM activation by MNNG in cells deficient for *NBS1* or *MSH6*. Msh6, as a subunit of MutS□, is required for the checkpoint response to methylated DNA (Stojic et al., 2004b; Wang and Qin, 2003). The results of a recent study indicate that Nbs1, in addition to its role in DSB-induced ATM activation, is required for the ATR-mediated Chk1 phosphorylation induced by HU or UV (Stiff et al., 2005). Consistent with the results of these studies, we found that MNNG-induced and ATR-mediated Chk1 phosphorylation is Nbs1- and Msh6-dependent (Fig. 1B and 1D). These findings establish that the Chk1 and Chk2 phosphorylation that is linked to methylated DNA damage requires the DNA damage sensors, Msh6 and Nbs1, in addition to early acting checkpoint proteins such as Rad17 and Rad9.

In contrast, we found that ATM is activated by MNNG in an Nbs1- and Msh6-independent manner (Fig. 1C and 1E), suggesting that, in addition to strict DNA damage-dependent ATR activation, MNNG activates ATM by mechanisms that do not require methylated DNA damage or DSB, which are potentially generated by damage to methylated DNA during DNA repair or replication. This result is consistent with the previous findings that agents that alter chromatin structure without introducing detectable DSB induce ATM autophosphorylation on Ser-1981 (Bakkenist and Kastan, 2003). However, this hypothesis does not necessarily rule out the possibility that the damage to methylated DNA is converted to DSB (Fig. 5C), the accumulation of which might result in abnormalities in the cellular redox state under conditions of ATM deficiency.

The results of our experiments using cells deficient for *NBS1* or *MSH6* suggest that ATM is directly activated by MNNG in the absence of DNA damage. Indeed, we found that ATM is activated by the direct treatment of chromatin-free immunoprecipitated ATM with MNNG, through the modification of critical SH groups (Fig. 2). However, it is possible that catalytic SH groups of ATM-

associated phosphatase-5 or phosphatase 2A (Ali et al., 2004; Goodarzi et al., 2004) are the actual targets of MNNG. To further explore the possible involvement of ATM's SH groups, we studied whether 15d-PGJ_2 activates ATM. 15d-PGJ_2 is a potent inducer of intracellular oxidative stress (Kondo et al., 2001) and directly modulates the activity of several biologically important molecules through the specific alkylation of free SH groups on cysteine residues of target proteins (Cernuda-Morollon et al., 2001; Oliva et al., 2003; Rossi et al., 2000; Shibata et al., 2003). We found that 15d-PGJ_2 effectively activated the kinase activity of ATM in both intact cells and immunoprecipitates (Fig. 3). Importantly, ATM activation was not induced with a 15d-PGJ_2 analog, 9,10-dihydro-15d-PGJ_2 (CAY, Fig. 3B), which lacks the reactive electrophilic α,β-unsaturated ketone that is involved in oxidative stress induction and SH-group reactivity (Shibata et al., 2003). Using biotinylated 15d-PGJ_2, we further demonstrated that 15d-PGJ_2 covalently binds to ATM through the alkylation of ATM's cysteine residues (Fig. 4). These results indicate that ATM is a direct target for 15d-PGJ_2, raising the interesting possibility that critical SH groups on ATM function as a direct oxidative stress sensor, independent of ATM's role in the cellular response to DSB.

Alternatively, it is plausible that free SH groups, together with Ser-1981, are involved in dormant dimer formation (Bakkenist and Kastan, 2003), and the modification of the SH groups and Ser-1981 autophosphorylation results in ATM dissociation and activation. This idea is consistent with the results of recent studies that suggest that ATM autophosphorylation is not sufficient for dimer dissociation and subsequent ATM activation (Goodarzi et al., 2004; Lee and Paull, 2005). We also found that, while 15d-PGJ_2 effectively activates ATM kinase activity (Fig. 3) and subsequent p53 phosphorylation and accumulation (Fig. 5A and 5C), 15d-PGJ_2 is not effective in ATM autophosphorylation (Fig. 5C). However, the formal establishment of these hypotheses requires the identification of the cysteine residues involved.

15d-PGJ_2 is a prostaglandin D_2 metabolite generated during inflammatory processes and is characterized by the presence of a reactive α,β-unsaturated ketone in the cyclopentenone ring, which functions as a potent inducer of intracellular oxidative stress (Gilroy et al., 1999; Kondo et al., 2001; Shibata et al., 2002). The results of immunohistochemical analysis indicate that 15d-PGJ_2 is detected

in foamy macrophages in human atherosclerotic plaques, lipopolysaaccharide-stimulated macrophages, inflammation-induced pleural exudates, or spinal cord tissues from patients with amyotrophic lateral sclerosis (Gilroy et al, 1999; Kondo et al, 2002; Shibata et al, 2002). Furthermore, 15d-PGJ_2 directly modulates the activity of several biologically important molecules, such as NF-□B, □□□ kinase, H-Ras, and thioredoxin, through the specific alkylation of free SH groups on cysteine residues in target proteins (Cernuda-Morollon et al., 2001; Oliva et al., 2003; Rossi et al., 2000; Shibata et al., 2003). In the present study, we demonstrated that ATM is another direct target of 15d-PGJ_2 (Fig. 3 and 4). However, in contrast to DSB-induced ATM activation, this 15d-PGJ_2-induced ATM activation is independent of Nbs1 and results in the phosphorylation and accumulation of p53 and in apoptosis, but does not cause the phosphorylation of Chk2 or H2AX (Fig. 5). This pattern of ATM activation by 15d-PGJ_2 is consistent with previous findings; although p53 phosphorylation and ATM autophosphorylation are Nbs1-independent, Chk2 phosphorylation is Nbs1-dependent and strictly linked to DNA damage (Falck et al., 2005; Kitagawa et al., 2004); agents that alter chromatin structure without introducing detectable DSB, induce ATM autophosphorylation but not H2AX phosphorylation (Bakkenist and Kastan, 2003). This pattern of ATM activation by 15d-PGJ_2 may be physiologically significant, considering the anti-inflammatory and pro-apoptotic roles that 15d-PGJ_2 plays in various disease states (Castrillo et al., 2000; Kondo et al., 2002; Lee et al., 2003; Straus and Glass, 2001). In particular, 15d-PGJ_2 has been implicated in p53-dependent neuronal apoptosis (Kondo et al, 2002). This pattern is also consistent with the observation that a portion of the extranuclear ATM localizes to peroxisomes (Watters et al., 1999). In addition, we recently showed that 4-oxo-2-nonenal, a major lipid peroxidation product, induces ATM autophosphorylation, p53 phosphorylation, and apoptosis in SH-SY5Y human neuroblastoma cells (Shibata et al., 2006). ATM, therefore, may function as an early monitor of various endogenously produced electrophilic metabolites and as a regulator of the cellular oxidative stress response to protect cells from the toxic effects of these metabolites, or to induce apoptosis. It is conceivable that the impairment of the ATM functions proposed here can eventually result in clinical manifestations of A-T, such as cerebellar ataxia, premature aging, growth retardation, or cancer.

Experimental procedures

Cell culture, reagents, and X-ray irradiation. DT40 cells were cultured in RPMI-1640 supplemented with 10% fetal calf serum (FCS), 1% chicken serum, 2 mM L-glutamine, 50 μg/ml penicillin, 50 units/ml streptomycin, and 10^{-5} M β-mercaptoethanol at 39.5˚C in a humidified 5% CO_2 incubator. The 293T, YZ5, EBS, and MCF7 cells were cultured in Dulbecco's modified Eagle medium (Nissui) supplemented with 15% FCS, 2 mM L-glutamine, 50 μg/ml penicillin, and 50 units/ml streptomycin. MNNG and NEM were obtained from Nacalai tesque and SIGMA, respectively. 15d-PGJ_2 and its analog, 9,10-dihydro-15d-PGJ_2 (CAY10410), were from Cayman Chemical. Biotinylated 15d-PGJ_2 was prepared as previously described (Shibata et al., 2003). X-ray irradiation was performed using an MBR-1520R radiator (Hitachi) set at 150-kVp, 20 mA, 0.5 mm aluminum, and 0.5 mm copper filtration with a dose rate of 1 Gy/min.

Gene targeting. A chicken EST clone (AI981357) containing the amino acid sequence homologous to human Msh6 was obtained at the NCBI web site. Oligonucleotide PCR primers were designed based on the EST clone, and partial chicken *MSH6* cDNA was amplified by RT-PCR using RNA extracted from DT40 cells. Using the cDNA fragment as a probe, chicken *MSH6* genomic clones were isolated from a spleen lambda genomic library (Stratagene). The identity of this clone was confirmed by DNA sequencing. *MSH6* targeting vectors were constructed by replacing exons 2-4 of the *MSH6* gene with his- and bsr-selection marker gene cassettes. For gene targeting of the chicken *MSH6* locus, wild-type DT40 cells were sequentially transfected with pMSH6-his and pMSH6-bsr (Supplementary Fig. 1), as previously described (Takao et al., 1999).

Antibodies. The 1.8-kbp DNA fragment was amplified by PCR using a partial chicken *ATM* cDNA fragment (Takao et al., 1999) as a template. The PCR fragment was treated with BamHI and KpnI, and the purified 600-bp fragment was then ligated to the BamHI- and KpnI-treated pQE31 (Qiagen), yielding His-tag-fused partial chicken *ATM* expression plasmids. This plasmid contains the chicken ATM amino acid sequence corresponding to the 1943-2124 amino acids of human ATM

(Supplementary Fig. 2). The His-tag ATM was purified with an Ni-NTA column (Qiagen) and was used to immunize white rabbits, and anti-ATM antisera were obtained from these rabbits. Antibodies against phospho-Chk1 (Ser-345), phospho-Chk2 (Thr-68), phospho-p53 (Ser-15), and phospho-ATM (ser-1981) were from Cell Signaling Technology. Antibodies against phospho-H2AX (Ser-139), Chk1, p53, ATM, and actin were from Upstate, Santa Cruz Biotechnology, Calbiochem, GeneTex, Inc., and Sigma, respectively.

GST-Rad9 fusion proteins. The expression vector for the GST-fused chicken Rad9 fragment containing the ATM phosphorylation site (Supplementary Fig. 3) was constructed as follows. A chicken *RAD9* DNA fragment was amplified by PCR using chicken *RAD9* cDNA (Kobayashi et al., 2004). The PCR fragment was treated with BamHI and XhoI, and the fragment was ligated into BamHI- and XhoI-treated pGEX4T-3 (Pharmacia Biotech), yielding a GST-Rad9 fusion protein expression plasmid. The GST-Rad9 fusion protein was purified with Glutathione Sepharose 4B (Pharmacia Biotech).

Immunoblot analysis. Cells were harvested, washed, and lysed in lysis buffer A (50 mM Tris-HCl (pH 7.5), 150 mM NaCl, 1% NP-40, 0.5% Na-deoxycholate, 0.1% SDS, 1 mM EDTA, 1 mM PMSF, 1 mM Na_3VO_4, 1 mM NaF, 1 □g/ml aprotinin, 1 □g/ml leupeptin). After centrifugation at 16,000 x g for 15 min, the protein concentrations of the cleared lysates were determined by the Bio-Rad protein quantification assay. The same amounts of protein were separated by SDS-PAGE (8 or 15%), followed by blotting to nitrocellulose or to a Hybond-P (Amersham Biosciences) membrane.

Immunoprecipitation (IP) kinase assay for ATM. Cells were treated with IR, MNNG, or 15d-PGJ_2 in a CO_2 incubator, then collected, washed with ice-cold PBS, and lysed in NETN150 (20 mM Tris-HCl (pH 8.0), 1 mM EDTA, 150 mM NaCl, 0.5% NP-40, 1 mM PMSF, 10 mM □–glycerophosphate, 1 mM NaF, 0.1 mM Na_3VO_4, 0.2 U/ml aprotinin, 10 □g/ml leupeptin, 5 □g/ml pepstatin). After clarifying the cell lysates by centrifugation, antibodies to chicken ATM were added to the extracts, and the reaction mixtures were rotated for 1 h at 4˚C, followed by incubation with protein G-Sepharose 4 Fast Flow (Amersham Biosciences) for 1 h at 4˚C. The immunoprecipitates were washed twice with lysis buffer and twice with kinase buffer (20 mM HEPES/KOH pH 7.5, 10 mM

$MgCl_2$, 10 mM $MnCl_2$). The immunoprecipitates thus prepared was not contaminated with chromatin components, as we could not detect Histone H3 in the immunoprecipates by immunoblot analysis (data not shown). After centrifugation, the immunoprecipitates were resuspended in 20 μl of kinase buffer containing 25 μM ATP, 1 μg GST-Rad9-fusion proteins, and 10 μCi of [γ-^{32}P]ATP. The reaction mixtures were incubated for 30 min at 30 ˚C, then boiled in SDS sample buffer for SDS-PAGE (13%). Gels were dried onto a filter paper and analyzed by autoradiography. Radioactivity was quantified with a Bio-image Analyzer BAS1000 (Fujix). In other experiments, immunoprecipitated ATM, prepared as described above, was mixed with 10 μl of MNNG or 15d-PGJ_2 diluted in kinase buffer and 10 μl of kinase buffer containing 50 μM ATP, 1 μg GST-Rad9 protein, and 10 μCi [γ-^{32}P]ATP. The reaction mixtures were incubated for 30 min at 30˚C, and the ATM kinase activity was measured as described above. For NEM treatment, immunoprecipitated ATM was resuspended in kinase buffer containing NEM and incubated for 15 min at 25˚C. The immunoprecipitates were washed once with kinase buffer, then used for the kinase assay.

Covalent binding of 15d-PGJ_2 to ATM. We isolated several partial and overlapping human *ATM* cDNA clones by library screening and PCR based on the published human *ATM* cDNA sequence (Savitsky et al., 1995), and a full-length *ATM* cDNA was constructed from these cDNA clones. The full-length human *ATM* cDNA expression vector with an HA-tag (HA-hATM) was prepared stepwise by constructing an HA-tagged eukaryotic expression vector, pEF-3HA, and then cloning the entire ATM coding sequence in the correct orientation into the expression vector, pEF-HA-hATM (the HA-tag sequence is located upstream of the ATM coding sequence). To prepare *ATM*$^{-/-}$ DT40 cells stably expressing a doxycycline-inducible *HA-hATM* gene (*ATM*$^{-/-}$/HA-hATM), we used pUHD10-1 and pUHD172-1neo plasmids (kindly provided by Dr. M. Gossen) (Gossen et al., 1995). *ATM*$^{-/-}$ DT40 cells were transfected with both the PvuI-digested pUHD10-3-HA-hATM and XhoI-digested pUHD172-1neo and selected with neomycin, yielding *ATM*$^{-/-}$/HA-hATM DT40 cells.

ATM$^{-/-}$/HA-hATM cells were incubated with doxycycline (1 μg/ml) overnight, collected, washed with ice-cold PBS, and lysed in lysis buffer B (50 mM Tris-HCl (pH 8.0), 100 mM NaCl, 0.5% Tween20, 0.2% NP-40, 1 mM PMSF, 0.2 U/ml aprotinin, 10 μg/ml leupeptin, 5 μg/ml pepstatin). After

clarifying the lysates by centrifugation, the extracts were reacted with an anti-HA antibody (Boehringer Mannheim) for 2 h at 4˚C. The reaction mixtures were then incubated with protein G-Sepharose 4 Fast Flow for 1 h at 4˚C. The immunoprecipitates were washed four times with lysis buffer B, and twice with reaction buffer (20 mM HEPES/KOH, pH 7.5). The immunoprecipitates were resuspended in 60 ml reaction buffer with or without 50 μM biotinylated 15d-PGJ_2, incubated for 1 h at 30˚C, then boiled in SDS sample buffer. The reaction products were separated by SDS-PAGE (6%) and biotinylated proteins were detected with HRP-conjugated NeutrAvidin (Pierce Biotechnology). For chicken ATM, anti-sera to chicken ATM and NETN150 supplemented with protease inhibitors were used instead of the anti-HA antibodies and lysis buffer B, respectively.

$ATM^{-/-}$/HA-hATM cells were incubated with doxycycline overnight, then incubated with or without 20 μM biotinylated 15d-PGJ_2 for 1 h in a CO_2 incubator. The cells were collected, washed with ice-cold PBS, and lysed in NETN150 supplemented with protease inhibitors. After centrifugation, the cleared extracts were incubated with 50 μl NeutrAvidin-Plus beads (PIERCE Biotechnology) for 3 h at 4˚C with rotation and shaking. After centrifugation, the supernatants were collected as the "Unbound" fractions. The beads were washed four times with the lysis buffer, and were boiled in SDS sample buffer to prepare the bound proteins ("Bound"). The "Unbound" and "Bound" proteins were separated by SDS-PAGE (6%), and HA-hATM was detected by using the anti-HA antibody as the primary antibody.

Assessment of apoptosis. YZ5 and EBS cells were untreated or treated with 40 μM of 15d-PGJ_2. After a 24-h incubation, the cells were trypsinized and harvested. Apoptotic cells were stained with annexin V using the Annexin V apoptosis kit (Clontech), and the annexin V–positive cells were detected by a FACS Calibur (Becton Dickinson), following the manufacturer's instructions.

Acknowledgments

We thank Dr. Y. Shiloh for the YZ5 and EBS cells, and Dr. M. Gossen for the pUHD10-1 and pUHD172-1neo plasmids. This work was supported in part by Grants-in-Aid from the Ministry of Education, Science and Culture of Japan.

References

Abraham, R.T. (2001) Cell cycle checkpoint signaling through the ATM and ATR kinases. *Genes Dev*, **15**, 2177-2196.

Adamson, A.W., Kim, W.J., Shangary, S., Baskaran, R. and Brown, K.D. (2002) ATM is activated in response to N-methyl-N'-nitro-N-nitrosoguanidine-induced DNA alkylation. *J Biol Chem*, **277**, 38222-38229.

Ali, A., Zhang, J., Bao, S., Liu, I., Otterness, D., Dean, N.M., Abraham, R.T. and Wang, X.F. (2004) Requirement of protein phosphatase 5 in DNA-damage-induced ATM activation. *Genes Dev*, **18**, 249-254.

Bakkenist, C.J. and Kastan, M.B. (2003) DNA damage activates ATM through intermolecular autophosphorylation and dimer dissociation. *Nature*, **421**, 499-506.

Barlow, C., Dennery, P.A., Shigenaga, M.K., Smith, M.A., Morrow, J.D., Roberts, L.J., 2nd, Wynshaw-Boris, A. and Levine, R.L. (1999) Loss of the ataxia-telangiectasia gene product causes oxidative damage in target organs. *Proc Natl Acad Sci USA*, **96**, 9915-9919.

Beardsley, D.I., Kim, W.J. and Brown, K.D. (2005) N-methyl-N'-nitro-N-nitrosoguanidine activates cell-cycle arrest through distinct mechanisms activated in a dose-dependent manner. *Mol Pharmacol*, **68**, 1049-1060.

Castrillo, A., Diaz-Guerra, M.J., Hortelano, S., Martin-Sanz, P. and Bosca, L. (2000) Inhibition of IkappaB kinase and IkappaB phosphorylation by 15-deoxy-Delta(12,14)-prostaglandin J(2) in activated murine macrophages. *Mol Cell Biol*, **20**, 1692-1698.

Cernuda-Morollon, E., Pineda-Molina, E., Canada, F.J. and Perez-Sala, D. (2001) 15-Deoxy-Delta 12,14-prostaglandin J2 inhibition of NF-kappaB-DNA binding through covalent modification of the p50 subunit. *J Biol Chem*, **276**, 35530-35536.

Chen, M.J., Lin, Y.T., Lieberman, H.B., Chen, G. and Lee, E.Y. (2001) ATM-dependent phosphorylation of human Rad9 is required for ionizing radiation-induced checkpoint activation. *J Biol Chem*, **276**, 16580-16586.

Falck, J., Coated, J. and Jackson, S.P. (2005) Conserved modes of recruitment of ATM, ATR and DNA-PKcs to sites of DNA damage. *Nature*, **434**, 605-611.

Gilroy, D.W., Colville-Nash, P.R., Chivers, D.W., Paul-Clark, M.J. and Willoughby, D.A. (1999) Inducible cyclooxygenase may have anti-inflammatory properties. *Nat Med*, **5**, 698-701.

Giuliano, P., De Cristofaro, T., Affaitati, A., Pizzulo, G.M., Feliciello, A., Criscuolo, C., G., D.M., Filla, A., Avvedimento, E.V. and S., V. (2003) DNA damege induced by polyglutamine-expanded proteins. *Hum Mol Genet*, **12**, 2301-2309.

Goodarzi, A.A., Jonnalagadda, J.C., Douglas, P., Young, D., Ye, R., Moorhead, G.B., Lees-Miller, S.P. and khanna, K.K. (2004) Autophosphorylation of ataxia-telangiectasia mutated is regulated by protein phosphatase 2A. *Embo J*, **23**, 4451-4461.

Gossen, M., Freundlieb, S., Bender, G., Muller, G., Hillen, W. and Bujard, H. (1995) Transcriptional activation by tetracyclines in mammalian cells. *Science*, **268**, 1766-1769.

Ito, K., Hirao, A., Arai, F., Matsuoka, S., Takubo, K., Hamaguchi, I., Nomiyama, K., Hosokawa, K., Sakurada, K., Nakagata, N., Ikeda, Y., Mak, T.W. and Suda, T. (2004) Regulation of oxidative stress by ATM is required for self-renewal of haematopoietic stem cells. *Nature*, **431**, 997-1002.

Johnson, B.F. and Greenberg, J. (1973) Modification of three enzymes of the beta-ketoadipate pathway by N-methyl-N'-nitro-N-nitrosoguanidine. *Chem Biol Interact*, **7**, 17-28.

Kamsler, A., Daily, D., Hochman, A., Stern, N., Shiloh, Y., Rotman, G. and Barzilai, A. (2001) Increased oxidative stress in ataxia telangiectasia evidenced by alterations in redox state of brains from Atm-deficient mice. *Cancer Res*, **61**, 1849-1854.

Kitagawa, R., Bakkenist, C.J., McKinnon, P.J. and Kastan, M.B. (2004) Phosphorylation of SMC1 is a critical downstream event in the ATM-NBS1-BRCA1 pathway. *Genes Dev*, **18**, 1423-1438.

Kobayashi, M., Hirano, A., Kumano, T., Xiang, S.L., Mihara, K., Haseda, Y., Matsui, O., Shimizu, H. and Yamamoto, K. (2004) Critical role for chicken Rad17 and Rad9 in the cellular response to DNA damage and stalled DNA replication. *Genes to Cells*, **9**, 291-303.

Kondo, M., Oya-Ito, T., Kumagai, T., Osawa, T. and Uchida, K. (2001) Cyclopentenone prostaglandins as potential inducers of intracellular oxidative stress. *J Biol Chem*, **276**, 12076-12083.

Kondo, M., Shibata, T., Kumagai, T., Osawa, T., Shibata, N., Kobayashi, M., Sasaki, S., Iwata, M., Noguchi, N. and Uchida, K. (2002) 15-Deoxy-Delta(12,14)-prostaglandin J(2): the endogenous electrophile that induces neuronal apoptosis. *Proc Natl Acad Sci USA*, **99**, 7367-7372.

Lee, J.H. and Paull, T.T. (2004) Direct activation of the ATM protein kinase by the Mre11/Rad50/Nbs1 complex. *Science*, **304**, 93-96.

Lee, J.H. and Paull, T.T. (2005) ATM activation by DNA double-strand breaks through the Mre11-Rad50-Nbs1 complex. *Science*, **308**, 551-554.

Lee, T., Tsai, H. and Chau, L. (2003) Induction of heme oxygenase-1 expression in murine macrophages is essential for anti-inflammatory effect of low dose 15-deoxy-Delta(12,14)-prostaglandin J2. *J Biol.Chem*, **278**, 19325-19330.

Morrison, C., Sonoda, E., Takao, N., Shinohara, A., Yamamoto, K. and Takeda, S. (2000) The controlling role of ATM in recombinational repair of DNA damage. *EMBO J*, **19**, 463-471.

Nagao, M., Hosoi, H. and Sugimura, T. (1971) Modification of cytochrome c with N-methyl-N'-nitro-N-nitrosoguanidine. *Biochim Biophys Acta*, **237**, 369-377.

Oliva, J.L., Perez-Sala, D., Castrillo, A., Martinez, N., Canada, F.J., Bosca, L. and Rojas, J.M. (2003) The cyclopentenone 15-deoxy-delta 12,14-prostaglandin J2 binds to and activates H-Ras. *Proc Natl Acad Sci USA*, **100**, 4772-4777.

Reitman, F.A., Shertzer, H.G. and Berger, M.L. (1988) Toxicity of methylating agents in isolated hepatocytes. *Biochem Pharmacol*, **37**, 3183-3188.

Rossi, A., Kapahi, P., Natoli, G., Takahashi, T., Chen, Y., Karin, M. and Santoro, M.G. (2000) Anti-inflammatory cyclopentenone prostaglandins are direct inhibitors of IkappaB kinase. *Nature*, **403**, 103-108.

Savitsky, K., Sfez, S., Tagle, D., Ziv, Y., Sartiel, A., Collins, F.S., Shiloh, Y. and Rotman, G. (1995) The complete sequence of the coding region of the ATM gene reveals similarity to cell cycle regulators in different species. *Hum. Mol. Genet.*, **4**, 2025-2032.

Shackelford, R.E., Innes, C.L., Sieber, S.O., Heinloth, A.N., Leadon, S.A. and Paules, R.S. (2001) The Ataxia telangiectasia gene product is required for oxidative stress-induced G1 and G2 checkpoint function in human fibroblasts. *J Biol Chem*, **276**, 21951-21959.

Shibata, T., Iio, K., Kawai, Y., Shibata, N., Kawaguchi, M., Toi, S., Kobayashi, M., Yamamoto, K. and Uchida, K. (2006) Identification of a lipid peroxidation product as a potential trigger of the p53 pathway. *J Biol Chem*, **in press**.

Shibata, T., Kondo, M., Osawa, T., Shibata, N., Kobayashi, M. and Uchida, K. (2002) 15-deoxy-delta 12,14-prostaglandin J2. A prostaglandin D2 metabolite generated during inflammatory processes. *J Biol Chem*, **277**, 10459-10466.

Shibata, T., Yamada, T., Ishii, T., Kumazawa, S., Nakamura, H., Masutani, H., Yodoi, J. and Uchida, K. (2003) Thioredoxin as a molecular target of cyclopentenone prostaglandins. *J Biol Chem*, **278**, 26046-26054.

Shiloh, Y. and Kastan, M.B. (2001) ATM: genome stability, neuronal development, and cancer cross paths. *Adv Cancer Res*, **83**, 209-254.

Soussi T, B.A., Kress M, Stehelin D, May P. (1988) Nucleotide sequnce of a cDNA encoding the chicken p53 nuclear oncoprotein. *Nucleic Acids Res*, **16**, 11383.

Stern, N., Hochaman, A., Zemach, N., Weizman, N., Hammel, H., Shiloh, Y., Rotman, G. and Barzilai, A. (2002) Accumulation of DNA damage and reduced levels of nicotine adenine dinucleotide in the brains of Atm-deficient mice. *J Biol Chem*, **277**, 602-608.

Stiff, T., Reis, C., Alderton, G.K., Woodbine, L., O'Driscoll, M. and Jeggo, P.A. (2005) Nbs1 is required for ATR-dependent phosphorylation events. *Embo J*, **24**, 199-208.
Stojic, L., Brun, R. and Jiricny, J. (2004a) Mismatch repair and DNA damage signalling. *DNA Repair*, **3**, 1091-1101.
Stojic, L., Mojas, N., Cejka, P., Di Pietro, M., Ferrari, S., Marra, G. and Jiricny, J. (2004b) Mismatch repair-dependent G2 checkpoint induced by low doses of SN1 type methylating agents requires the ATR. kinase. *Genes Dev*, **18**, 1331-1344.
Straus, D.S. and Glass, C.K. (2001) Cyclopentenone prostaglandins: new insights on biological activities and cellular targets. *Med Res Rev*, **21**, 185-210.
Sugimura, T., Fujimura, S., Nagao, M., Yokoshima, T. and Hasegawa, M. (1968) Reaction of N-methyl-N'-nitro-N-nitrosoguanidine with protein. *Biochim Biophys Acta*, **170**, 427-429.
Takao, N., Kato, H., Mori, R., Morrison, C., Sonada, E., Sun, X., Shimizu, H., Yoshioka, K., Takeda, S. and Yamamoto, K. (1999) Disruption of ATM in p53-null cells causes multiple functional abnormalities in cellular response to ionizing radiation. *Oncogene*, **18**, 7002-7009.
Takao, N., Li, Y. and Yamamoto, K. (2000) Protective roles for ATM in cellular response to oxidative stress. *FEBS Lett*, **472**, 133-136.
Tauchi, H., Kobayashi, J., Morishima, K., van Gent, D.C., Shiraishi, T., Verkaik, N.S., vanHeems, D., Ito, E., Nakamura, A., Sonoda, E., Takata, M., Takeda, S., Matsuura, S. and Komatsu, K. (2002) Nbs1 is essential for DNA repair by homologous recombination in higher vertebrate cells. *Nature*, **420**, 93-98.
Uziel, T., Lerenthal, Y., Moyal, L., Andegeko, Y., Mittelman, L. and Shiloh, Y. (2003) Requirement of the MRN complex for ATM activation by DNA damage. *Embo J*, **22**, 5612-5621.
Wang, Y. and Qin, J. (2003) MSH2 and ATR form a signaling module and regulate twobranches of the damage response to DNA methylation. *Proc Natl Acad Sci USA*, **100**, 15387-15392.
Watters, D., Kedar, P., Spring, K., Bjorkman, J., Chen, P., Gatei, M., Birrell, G., Garrone, B., Srinivasa, P., Crane, D.I. and Lavin, M.F. (1999) Localization of a portion of extranuclear ATM to peroxisomes. *J Biol Chem*, **274**, 34277-34282.
Zhang, Y., Ma, W.Y., Kaji, A., Bode, A.M. and Dong, Z. (2002) Requirement of ATM in UVA-induced signaling and apoptosis. *J Biol Chem*, **277**, 3124-3131.
Ziv, Y., Bar-Shira, A., Pecker, I., Russell, P., Jorgensen, T.J., Tsarfati, I. and Shiloh, Y. (1997) Recombinant ATM protein complements the cellular A-T phenotype. *Oncogene*, **15**, 159-167.

Figure legends

Fig. 1. MNNG activates the ATM kinase in an Nbs1- and Msh6-independent manner. (A) Wild-type DT40 cells were treated with the indicated concentrations of MNNG for 1 h and the ATM kinase activity was measured. “C” indicates the control treated with DMSO, the MNNG solvent. (B) Wild-type (WT) and *NBS1*$^{-/-}$ DT40 cells were treated with 200 μM of MNNG for the indicated times, and the cell extracts were subjected to immunoblot analysis with anti-phospho-Chk1 (Ser-345) (upper panel), anti-phospho-Chk2 (Thr-68) (middle panel), and anti-Chk1 (lower panel) antibodies. (C) *NBS1*$^{-/-}$ DT40 cells were treated with the indicated concentrations of MNNG for 1 h. Cell extracts were prepared for the ATM kinase assay. (D) Wild-type and *MSH6*$^{-/-}$ DT40 cells were treated with 200 μM of MNNG for the indicated times, and cell extracts were subjected to immunoblot analysis with anti-phospho-Chk1 (Ser-345) (upper panel), anti-phospho-Chk2 (Thr-68) (middle panel), and anti-Chk1 (lower panel) antibodies. (E) *MSH6*$^{-/-}$ DT40 cells were treated with the indicated concentrations

of MNNG for 1 h, and the ATM kinase activity was measured.

Fig. 2. ATM is directly activated by MNNG through the modification of free SH groups. (A) Immunoprecipitated ATM prepared from untreated wild-type DT40 cells with anti-chicken ATM antibodies was mixed with 10 μl of various concentrations of MNNG and 10 μl of kinase buffer containing 50 μM ATP, 1 μg GST-Rad9-fragment, and 10 μCi of [γ-^{32}P]ATP. The mixtures were incubated for 30 min at 30˚C. The reaction products were subjected to SDS-PAGE followed by autoradiography. (B) Immunoprecipitated ATM was resuspended in kinase buffer containing the indicated concentrations of NEM and incubated for 15 min at 25˚C. The immunoprecipitated ATM was then washed once with kinase buffer, and subjected to MNNG treatment (0.5 μM) followed by the ATM kinase assay.

Fig. 3. ATM kinase activation by 15d-PGJ$_2$. (A) Wild-type DT40 cells were treated with the indicated concentrations of 15d-PGJ$_2$ for 1 h. The cells were harvested for the IP ATM kinase assay. "IB" indicates the relative amount of ATM in each extract. (B) Wild-type DT40 cells were untreated (C) or treated with methyl acetate (MA, the 15d-PGJ$_2$ solvent), 20 μM 15d-PGJ$_2$ (P), or 20 μM 9,10-dihydro-15d-PGJ$_2$ (CAY) for 1 h. The treated cells were then used for the IP ATM kinase assay. (C) Immunoprecipitated ATM prepared from untreated wild-type DT40 cells with anti-chicken ATM antibodies was subjected to 15d-PGJ$_2$ treatment, followed by the ATM kinase assay.

Fig. 4. Direct binding of 15d-PGJ$_2$ to ATM. (A) Immunoprecipitated chicken ATM prepared from wild-type (WT) and *ATM*$^{-/-}$ DT40 cells with anti-chicken ATM antibodies was incubated with or without 50 μM biotinylated 15d-PGJ$_2$. After incubation for 1 h at 30˚C, the immunoprecipitates were washed thoroughly, and immunoblotted with HRP-conjugated NeutrAvidin. (B) *ATM*$^{-/-}$/HA-hATM DT40 cells were incubated with or without doxycycline (Dox) overnight, and immunoprecipitated HA-tagged human ATM (HA-hATM) was prepared with anti-HA antibodies. The immunoprecipitates were then treated with biotinylated 15d-PGJ$_2$, and immunoblotted with HRP-conjugated NeutrAvidin. (C) *ATM*$^{-/-}$/HA-hATM DT40 cells were incubated with doxycycline overnight and incubated with or without 20 μM biotinylated 15d-PGJ$_2$ for 1 h. The cell extracts were then incubated with NeutrAvidin Plus for 3 h at 4˚C. The NeutrAvidin- "Bound" and "Unbound" fractions were used for immunoblot analysis with anti-HA antibodies.

Fig. 5. 15d-PGJ$_2$ induces p53 phosphorylation and apoptosis in an ATM-dependent manner. (A) EBS (ATM-deficient) and YZ5 (hATM-complemented) cells were treated with the indicated concentrations of 15d-PGJ$_2$ or 100 μM MNNG (M) for 1 h. Cell extracts were immunoblotted with

anti-phospho-Chk2 (Thr-68) (upper panel), anti-phospho-p53 (Ser-15) (middle panel), and anti-actin (lower panel) antibodies. (B) YZ5 and EBS cells were untreated (C), treated with 50 μM MNNG (M), or exposed to 15 Gy IR (IR). After a 1-h incubation, cell extracts were prepared and used for immunoblot analysis. (C) MCF7 cells were untreated (C) or treated with the indicated concentrations of 15d-PGJ_2 or MNNG for 4 h. Cell extracts were immunoblotted with anti-phospho-p53 (Ser-15), anti-p53, anti-phospho-ATM (Ser-1981), anti-ATM, anti-phospho-H2AX (Ser-139), and anti-actin antibodies. (D) YZ5 and EBS cells were untreated (open bar) or treated with 40 μM 15d-PGJ_2 (closed bar). After a 24-h incubation, the cells were trypsinized and harvested. Apoptotic cells were quantified by annexin V FACS analysis. Each value represents the mean + SD for at least three experiments.

Figure 1

A.

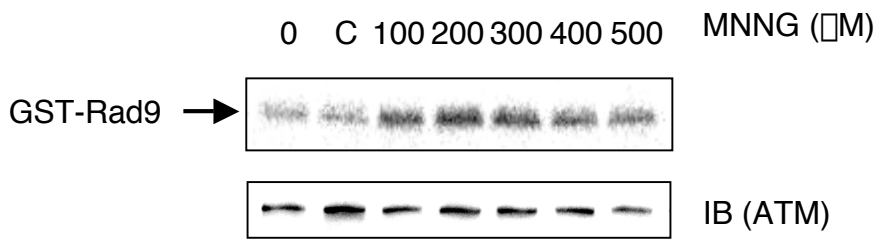

B.

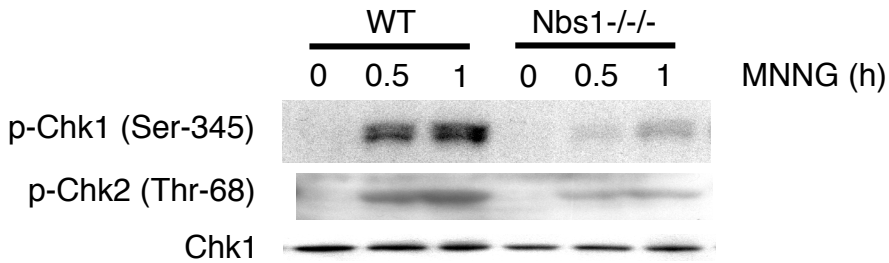

C.

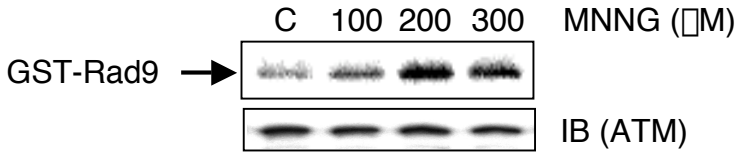

D.

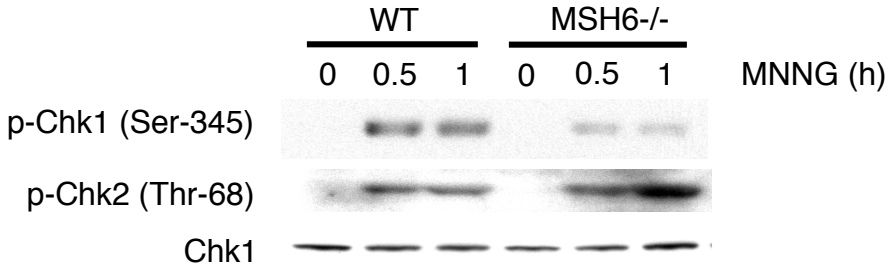

E.

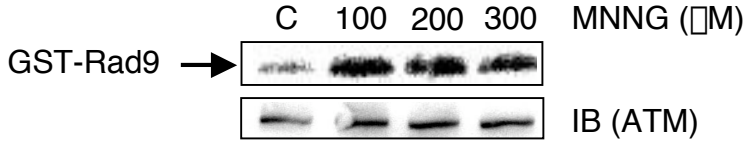

Figure 2

A.

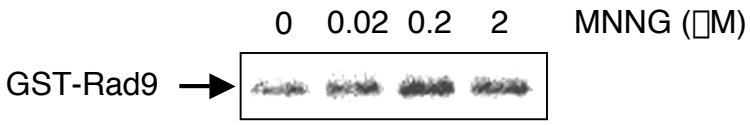

B.

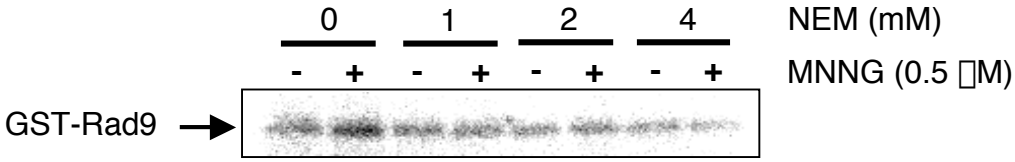

Figure 3

A.

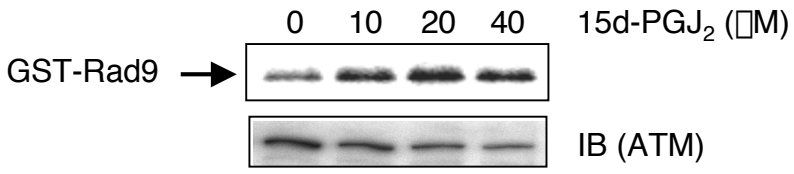
0 10 20 40
15d-PGJ2 (□M)
GST-Rad9
IB (ATM)

B.

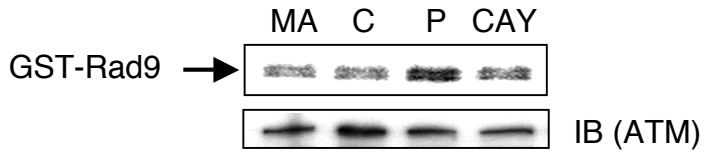
MA C P CAY
GST-Rad9
IB (ATM)

C.

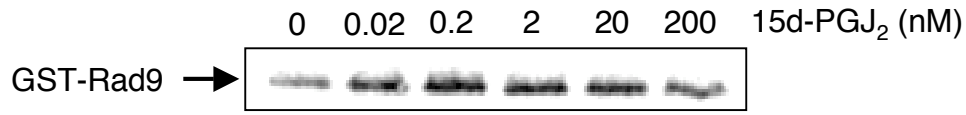
0 0.02 0.2 2 20 200
15d-PGJ2 (nM)
GST-Rad9

Figure 4

A.

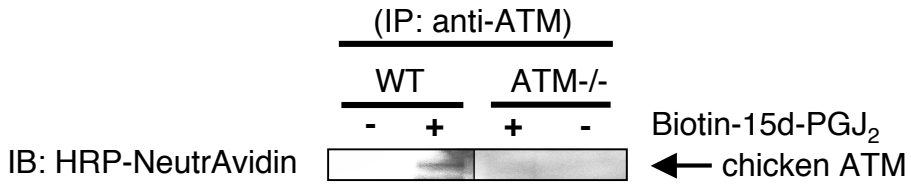
(IP: anti-ATM)
WT
ATM-/-
- + + -
Biotin-15d-PGJ2
IB: HRP-NeutrAvidin
chicken ATM

B.

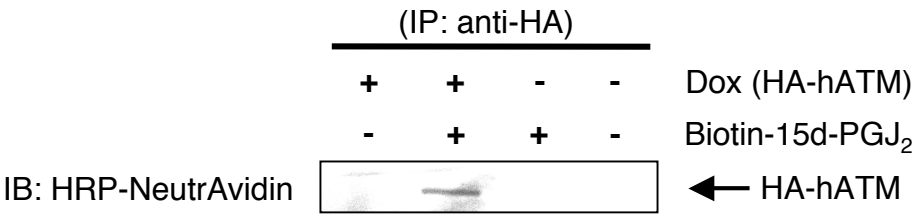
(IP: anti-HA)
+ + - - Dox (HA-hATM)
- + + - Biotin-15d-PGJ2
IB: HRP-NeutrAvidin
HA-hATM

C.

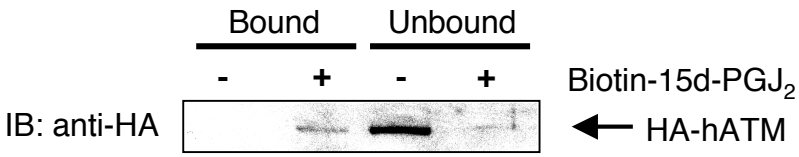
Bound
Unbound
- + - + Biotin-15d-PGJ2
IB: anti-HA
HA-hATM

Figure 5

A.

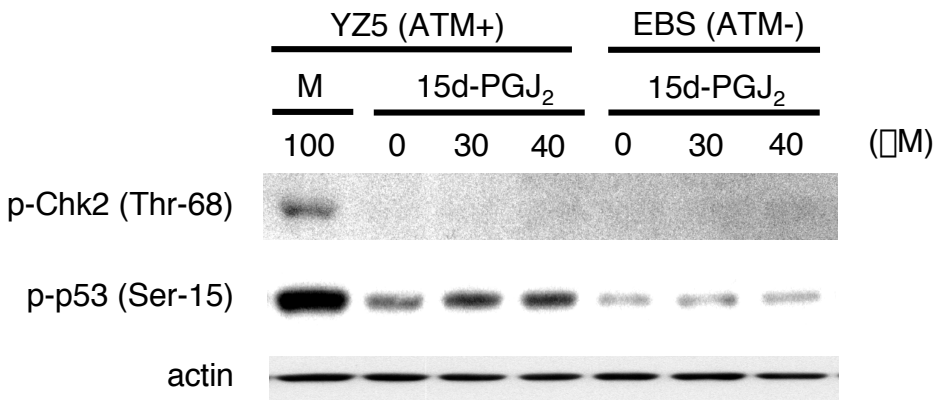
YZ5 (ATM+)
EBS (ATM-)
M
15d-PGJ2
15d-PGJ2
100
0
30
40
0
30
40
(M)
p-Chk2 (Thr-68)
p-p53 (Ser-15)
actin

B.

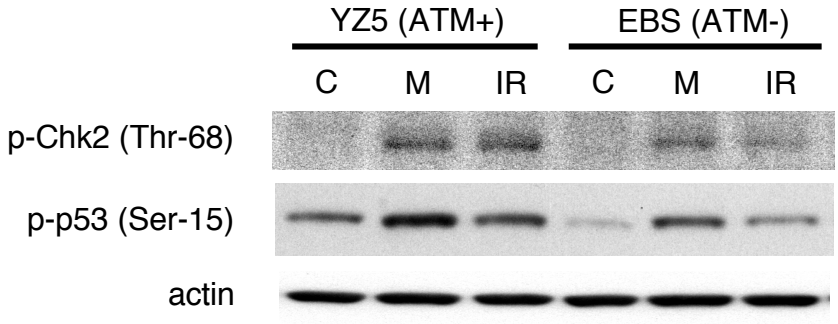
YZ5 (ATM+)
EBS (ATM-)
C
M
IR
C
M
IR
p-Chk2 (Thr-68)
p-p53 (Ser-15)
actin

C.

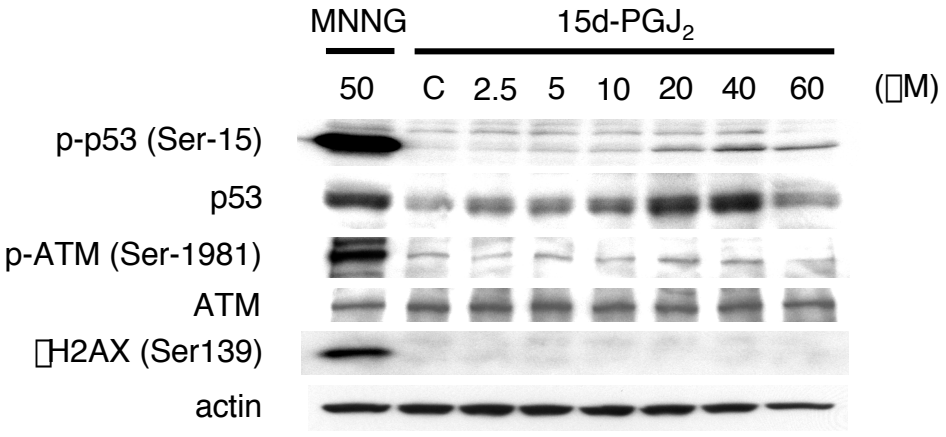
MNNG
15d-PGJ2
50
C
2.5
5
10
20
40
60
(M)
p-p53 (Ser-15)
p53
p-ATM (Ser-1981)
ATM
H2AX (Ser139)
actin

Figure 5

D.